Power Electronics and Drives

Multi-Criteria Decision Analysis Approach for DC Microgrid Bus Selection

Research Paper

Foued Charaabi*, Mehdi Dali, Jamel Belhadj

University of Tunis, National Higher School of Engineers of Tunis (ENSIT), Electrical Systems Laboratory (LSE), 1008 Tunis, Tunisia

Received: 03 March, 2025; Received in the revised form: 25 April, 2025; Accepted: 15 May, 2025

Abstract: The increasing variety of DC microgrid configurations has created a challenge for engineers in selecting the optimal design. To address this, multi-criteria decision analysis (MCDA) provides a systematic approach. In this study, six distinct DC microgrid configurations are defined as potential alternatives: unipolar, bipolar, multi-terminal topology, multi-bus topology, ring topology and AC microgrid. MCDA allows for the establishment of relevant evaluation criteria specific to each configuration, such as protection schemes, fault resilience and overall system cost. By systematically analysing the MCDA results using the analytic hierarchy process (AHP) technique, the most suitable DC microgrid design can be identified, which inherently determines the optimal type of distribution bus. AHP assigns weights to each evaluation criterion based on its relative importance. This study concludes with a comprehensive sensitivity analysis and an investigation of optimisation techniques. This assessment integrates perspectives from both expert judgements and relevant scientific publications.

Keywords: *DC Microgrid configurations • resilience • cost • MCDA • sensitivity*

1. Introduction

Many countries are encouraging people to use their individual microgrids by offering financial help (grants, tax discounts and payments for extra energy). They also provide education through workshops and awareness programs. These efforts help people to adopt microgrid technology, leading to a cleaner and more independent energy. With the increasing presence of prosumers, DC microgrids become a necessity. However, choosing the optimal topology requires collaboration. Producers and consumers can work together by identifying consumer priorities: maximizing self-consumption, minimizing grid reliance or prioritizing outage resilience. This approach, fostering a shared effort, empowers prosumers with DC microgrids, paving the way for a more sustainable energy future.

Tunisia, like many countries, is experiencing a growing trend towards consumer-producer model, the concept of individuals or communities both producing and consuming electricity, often through renewable energy sources, such as solar panels. This transfer necessitates a move from traditional grid structures to decentralised DC microgrids. However, implementing these microgrids effectively requires supportive policies for self-consumption and self-production. Tunisia has embarked on the path towards distributed energy generation. Further policy adjustments can significantly accelerate progress. Changing from the current net metering system to feed-in tariffs, as successfully implemented in Germany. Additionally, reorganising the permitting process for solar installations would reduce bureaucratic hurdles (Böhringer et al., 2017; Meddeb et al., 2018).

Financial support mechanisms, such as grants or tax breaks, can significantly lower upfront costs and encourage wider adoption of solar panels and microgrid integration. By implementing these targeted policy changes, Tunisia

* Email: charaabi.foued@gmail.com

can unlock the full potential of distributed energy generation and pave the way for a more decentralised and sustainable energy. The increasing transition to microgrids has introduced a diverse range of AC and DC microgrid topologies. This variety presents a challenge when it comes to selecting the optimal bus configuration, as multiple criteria need to be considered for effective decision-making (Feng et al., 2018).

Multi-criteria decision analysis (MCDA) methods are widely used in energy systems to support decisions involving multiple conflicting criteria. Among them, the analytic hierarchy process (AHP) is recognised for its clarity, flexibility and ability to integrate expert judgement with quantitative data. Recent studies emphasise the use of scientific data to reduce bias and enhance decision reliability (Parvaneh and Hammad, 2024).

The core of this study is structured into four main parts. The first part presents a comparison between unipolar and bipolar DC microgrids using two criteria cost and resilience, highlighting the trade-off between them. Improving resilience often leads to increased cost, making it difficult to determine the best configuration. The second part expands the analysis by evaluating six DC microgrid topologies with three criteria, aiming to provide a broader and more balanced decision framework. The third part is dedicated to sensitivity analysis, which examines the impact of small changes in criteria weights on the ranking of alternatives. The fourth part introduces an objective function designed to improve sensitivity performance, optimise the decision vector, and enhance the stability of the alternative rankings.

2. Resilience and Cost Analysis

Cost and resilience are closely linked, particularly in DC microgrids. Enhancing resilience by incorporating components, such as circuit breakers and additional battery storage, can lead to increased costs. On the contrary, minimizing costs may result in reduced resilience, making the system more vulnerable to disruptions. The main objective is to achieve an optimal balance where resilience is maximised within acceptable cost constraints. In the next study, each criterion will be analysed in detail for both unipolar and bipolar DC microgrid configurations to provide a comprehensive assessment of their advantages and limitations.

2.1. Topologies

DC microgrids can use unipolar or bipolar topologies. The unipolar DC bus is cost-effective but loses power delivery during faults, while the bipolar DC bus improves reliability by ensuring power delivery even during faults. The schematic of each microgrid topology is given in Figure 1, and the key bus characteristics are summarised in Table 1.

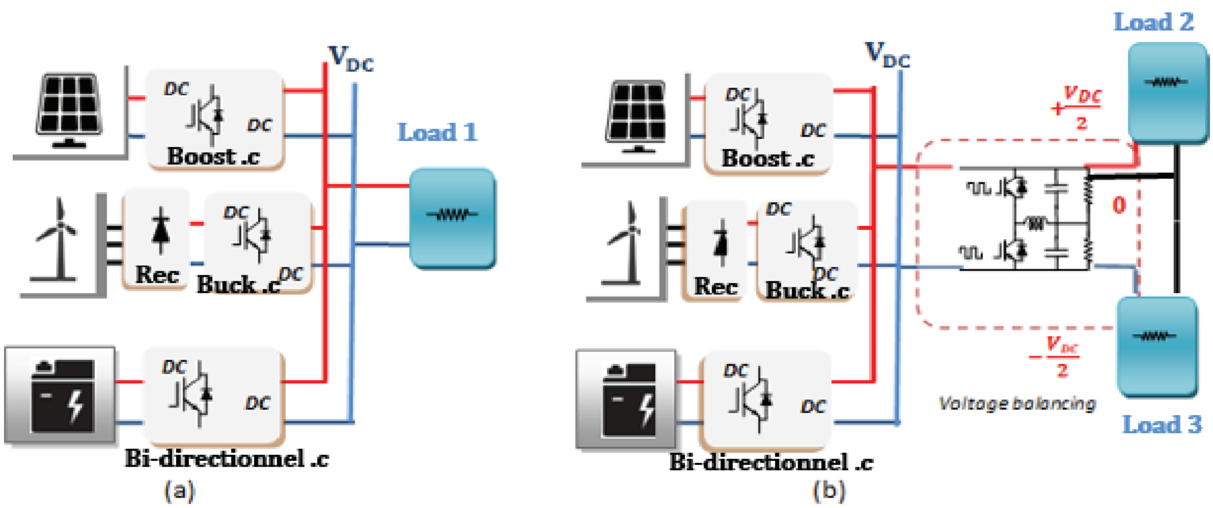

Figure 1. Unipolar (a) and bipolar (b) DC microgrid.

2.2. Microgrid resilience

The resilience of a microgrid can be evaluated according to three main elements. First, the resilience to source failure, which measures the system's ability to maintain power supply in the event of a power source failure. The second element is resilience to load variations, which evaluates the system's ability to adapt to fluctuations in energy demand. Finally, the resilience to disruptive events, such as short circuits, can lead to blackouts in certain configurations. This classification is provided in Figure 2.

Power system resilience can be evaluated through distinct phases, as shown in Figure 3. While the specific terminology used might vary across studies, the core concept of the resilience trapezoid represents two key phases: the disruption transition (td–ts) refers to the period from the start of the event to the end of its disruptive impact. The recovery transition phase (ts–tr) represents the duration from the beginning of restoration activities until the system fully regains functionality (Kiptoo et al., 2023).

Table 1. Microgrids and bus characteristics

Topology	Unipolar DC microgrid	Bipolar DC microgrid
Bus parameters	Single positive rail and ground	Positive, neutral and negative rails
Bus voltage	Single voltage (positive to ground)	Three-wire voltage (positive, neutral and negative)
Bus complexity	Simpler, with fewer components	More complex, with more components for balancing
Protection	Simple overcurrent/short-circuit protection	More complex, requiring balancing and fault detection for both rails
Voltage levels	300 V	±200 V
Power of sources	Pv (2 kW), wind (1 kW)	Pv (2 kW), wind (1 kW)
Load options	One voltage level per load, Load 1 (2 kW)	Load 2 (1 kW), load 3 (1 kW)

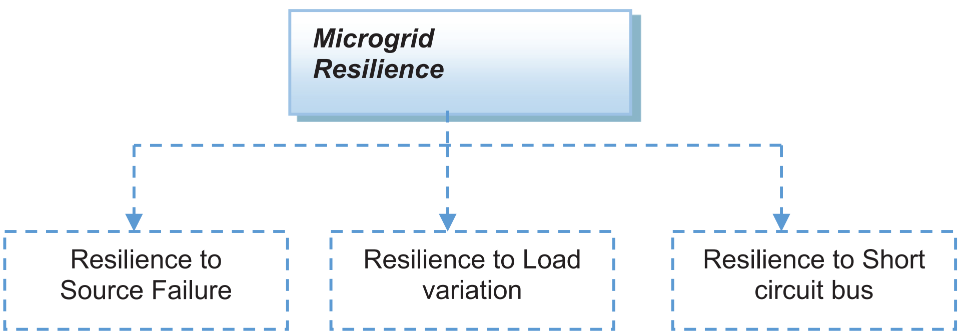

Figure 2. Microgrid resilience classification.

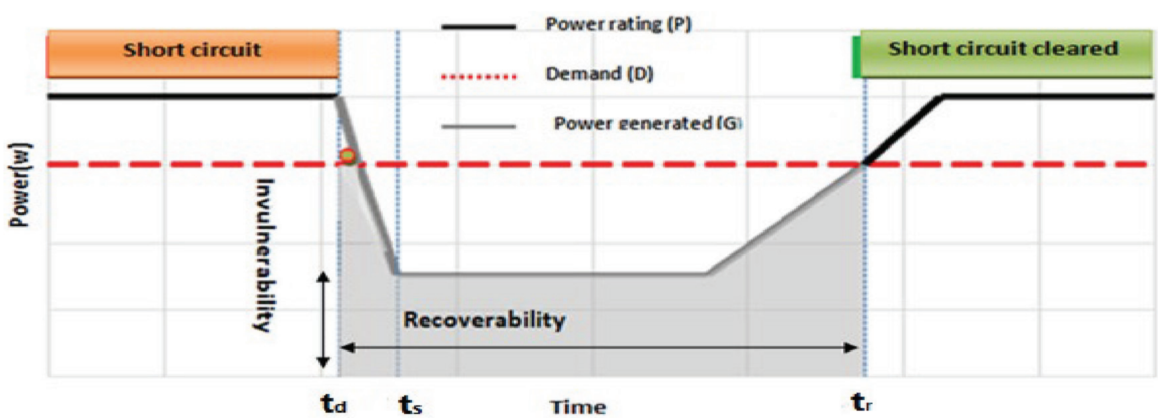

Figure 3. Resilience curve.

Invulnerability refers to the microgrid's ability to maintain operation during disturbances, as given by Eq. (1) (Beyza and Yusta, 2021; Wang et al., 2025).

$$\text{invulnerability} = \frac{P_{\text{microgrid}_{t_s}}}{P_{\text{microgrid}_{td}}} \tag{1}$$

where $P_{\text{microgrid}_{t_s}} = P_{\text{bat}} + P_{\text{pv}} + P_{\text{wind}}$ represents the rated power of the microgrid after a power disruption, and $P_{\text{microgrid}_{t_d}}$ is the power of the microgrid before disruption.

Recoverability indicates how quickly a microgrid can recover and resume full operation after a disruption, as represented by Eq. (2) (Yodo and Wang, 2016).

$$\text{recoverability} = 1 - \frac{\sum_{t=t_d}^{t=\text{t}_r} \left(P_{\text{load}} - P_{\text{ren}}\right)(t)}{\sum_{t=t_d}^{t=t_r} P_{\text{load}}(t)} \tag{2}$$

where P_{load} is the power demand and P_{ren} is the power generated by the PV (photovoltaic panel) and wind generators.

The overall resilience of the microgrid (MG) can be represented by Eq. (3) (Chang et al., 2021).

$$\text{Resilience} = (\text{invulnerability} + \text{ recoverability})/2 \tag{3}$$

To assess the resilience of the microgrid under short-circuit fault conditions, it is assumed that power generation remains constant and the load capacity is sufficient. By simulating a pole-to-ground fault on the bus, the investigation can evaluate the impact on each microgrid's invulnerability and recoverability (Rocchetta et al., 2018).

$$\text{invulnerability} = \begin{cases} 0 < \text{invulnerability} < 1 & \text{healthy bus} \\ 0 & \text{short circuit bus} \end{cases} \tag{4}$$

During a short-circuit fault, no power is delivered to the faulted branch, and recoverability is zero.

$$\text{recoverability} = 1 - \frac{\sum_{t=t_d}^{t=t_r} \left(\text{P}_{\text{load}_\text{t}}\right)}{\sum_{t=t_d}^{t=t_r} \text{P}_{\text{load}_\text{t}}} = 1 - 1 = 0 \tag{5}$$

In normal operating conditions, power is distributed efficiently and recoverability remains at its maximum.

$$\text{recoverability} = \begin{cases} \text{recoverability} = 1 & \text{healthy bus} \\ 0 & \text{short circuit bus} \end{cases} \tag{6}$$

In a system with two buses, such as a bipolar DC microgrid, the resilience can be expressed as:

$$R_{\text{bipolar MG}} = (R_{\text{bus1}} + R_{\text{bus2}})/2 \tag{7}$$

Bipolar DC microgrid architecture is more fault-resilient than unipolar DC microgrids, making it the superior choice between the two configurations.

2.3. Cost analysis

Table 2 compares the components, costs, and system specifications of unipolar and bipolar DC microgrids.

The annual cost of all components in the unipolar and bipolar DC microgrid is presented by Eqs. (8) and (9).

$$C_{t(annual)unipolar} = \sum_{pv=1}^{n_{pv}} (pv) + \sum_{wind=1}^{n_{wind}} (wind) + \sum_{c=1}^{n_c} (conv) + \sum_{b=1}^{n_b} (bat) + \sum_{i=1}^{2} \text{cost}_{\text{cable}} + \sum_{i=1}^{1} (\text{breaker}) \tag{8}$$

Table 2. Cost component comparison (Eskander and Silva, 2023; Jena et al., 2021)

Component / Topology	PV (2 kW)	Wind (1 kW)	Boost	Buck	AC/DC	Bid- conv	Balancer converter	Circuit breaker	Cables (3 kW)	Total cost
Unipolar DC MG (3 kW)	€2,000 (CS6K-300)	€2,500 (Bergey Excel)	€350 (Energy Skylla)	€200 (MeanWell)	€800 (SMA Sunny Island)	€800 (SMA Sunny Island)	Not required	€150 (ABB S202)	€200 (Sola Cable)	€6,150
Bipolar DC MG (3 kW)	€2,000 (CS6K-300)	€2,500 (Bergey Excel)	€350 (E. Skylla)	€200 (MeanWell)	€800 (SMA Sunny Island)	€800 (SMA Sunny Island)	€600 (Victron Energy BMV-702)	€150 (ABB S202)	€200 (Solar Cable)	€11,07

$$C_{t(\text{annual})\text{bipolar}} = \sum_{pv=1}^{n_{pv}}(\text{pv}) + \sum_{\text{wind}=1}^{n_{\text{wind}}}(\text{wind}) + \sum_{c=1}^{n_c}(\text{conv}) + \sum_{b=1}^{n_b}(\text{bat}) + \sum_{i=1}^{3}\text{cost}_{\text{cable}} + \sum_{i=1}^{2}(\text{breaker}) + \text{Cost}_{\text{circuit balancer}} \tag{9}$$

By calculating the ratio of the two annual costs, the relative economic performance of the unipolar and bipolar DC microgrids can be determinate by Eq. (10).

$$\frac{C_{t(\text{annual})\text{bipolar}}}{C_{t(\text{annual})\text{unipolar}}} = 1 + \frac{\text{Cost}_{\text{cable}}}{C_{t(\text{annual})\text{unipolar}}} + \frac{\text{Cost}_{\text{circuit balancer}}}{C_{t(\text{annual})\text{unipolar}}} + \frac{\text{Cost}_{\text{one breaker}}}{C_{t(\text{annual})\text{unipolar}}} \tag{10}$$

It is notable that the cost ratio is greater than one and can even reach two, depending on the specific technologies chosen for cables, breakers, and circuit balancers. A ratio approaching two indicates that bipolar DC microgrids are approximately twice as expensive to implement as unipolar ones.

The previous results were evaluated using HOMER (Hybrid Optimization of Multiple Energy Resources) software, UL Solutions (Formerly developed by HOMER Energy), which performs analysis based on net present cost (NPC) and cost of energy (COE). The analysis shows that the most cost-efficient configuration is a DC microgrid with only DC loads, as it achieves the lowest NPC and COE, as presented in Figure 4.

In conclusion, choosing the best microgrid configuration involves a trade-off between resilience and cost. If resilience is the priority, the bipolar DC microgrid is the optimal choice due to its ability to isolate faults and maintain partial functionality during short-circuit events. However, when cost is the primary concern, the unipolar DC microgrid becomes a more attractive option. The decision on which microgrid to adopt should be based on an analytical approach that balances these conflicting criteria. In this context, advanced methods such as the AHP can offer valuable insights.

3. Methodology

The AHP is a widely used multi-criteria decision-making (MCDM) methodology developed by Thomas Saaty in the 1970s. It helps analyse complex decisions by facilitating the prioritisation of alternatives and the identification of the optimal choice through pair-wise comparisons. By incorporating the weighted criteria of multiple experts, AHP reduces bias and ensures impartiality in the decision-making process. A review of the different steps in the AHP is provided in Figure 5 (Mohamed et al., 2019; Yodo and Wang, 2016).

3.1. AHP method

Table 3 presents a comparison of key DC and AC microgrid topologies, describing their characteristics, usage frequency. This comparison helps to identify the most appropriate topologies for the current evaluation. Six major microgrid topologies (AC, unipolar DC, bipolar DC, multi-terminal DC, multi-bus DC and ring DC) are selected for comparison based on their significance in existing literature and real-world applications. The remaining three topologies (radial DC, mesh DC and star DC) are excluded due to their limited usage and minimal practical relevance in contemporary microgrid systems (Saaty, 2008).

The AHP hierarchy foundation is composed of three phases, the initial phase defines the overall problem or decision goal at the top of the hierarchy. Below this, relevant criteria are identified and arranged in a hierarchical structure. The last step presents the different alternatives, as presented in Figure 6 (Kiptoo et al., 2023; Parvaneh and Hammad, 2024).

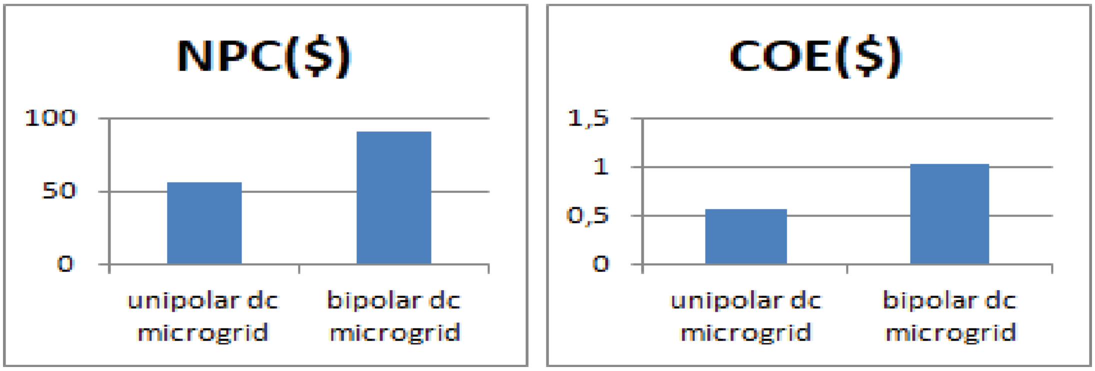

Figure 4. NPC and COE comparison. COE, cost of energy; NPC, net present cost.

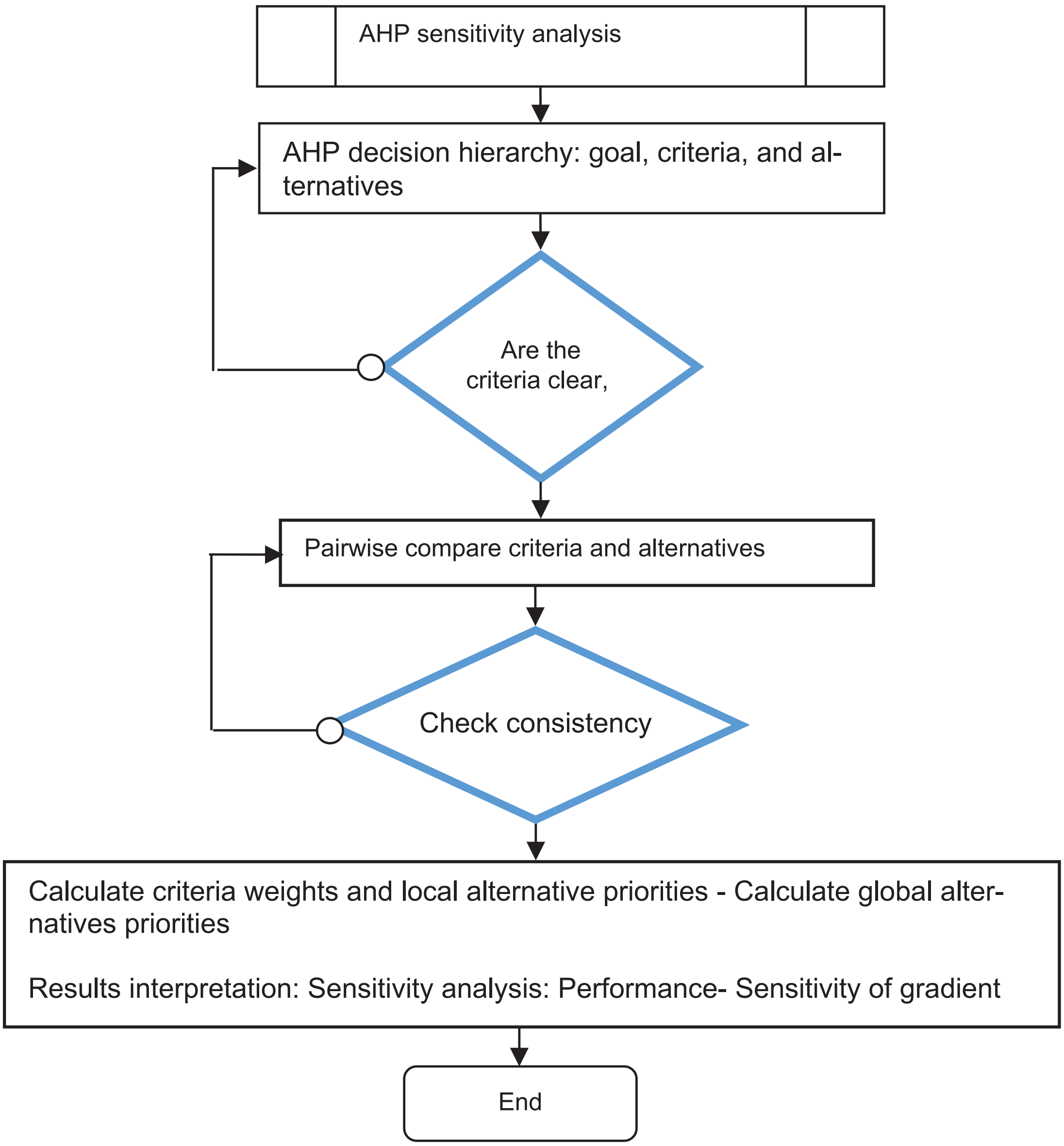

Figure 5. AHP technique process. AHP, analytic hierarchy process.

Table 3. Microgrids in the literature (Kumar and Prabha, 2022; Punitha et al., 2024)

Topology	Type	Characteristics	Usage frequency (%)
AC microgrid	AC	Standard, widely used, less efficient for DC systems	25
Unipolar DC microgrid	DC	Simple, low-cost, suitable for small-scale systems	13
Bipolar DC microgrid	DC	More reliable, reduces losses compared to unipolar	12
Multi-terminal DC	DC	Connects multiple sources and loads, modular	11
Multi-bus DC	DC	Flexible load distribution and efficient control	10
Ring DC	DC	High resilience, continuous power supply	10
Radial DC	DC	Simple, but vulnerable to faults; low redundancy	5
Mesh DC	DC	High reliability, but complex control	4
Star DC	DC	Centralised, best for small systems	3

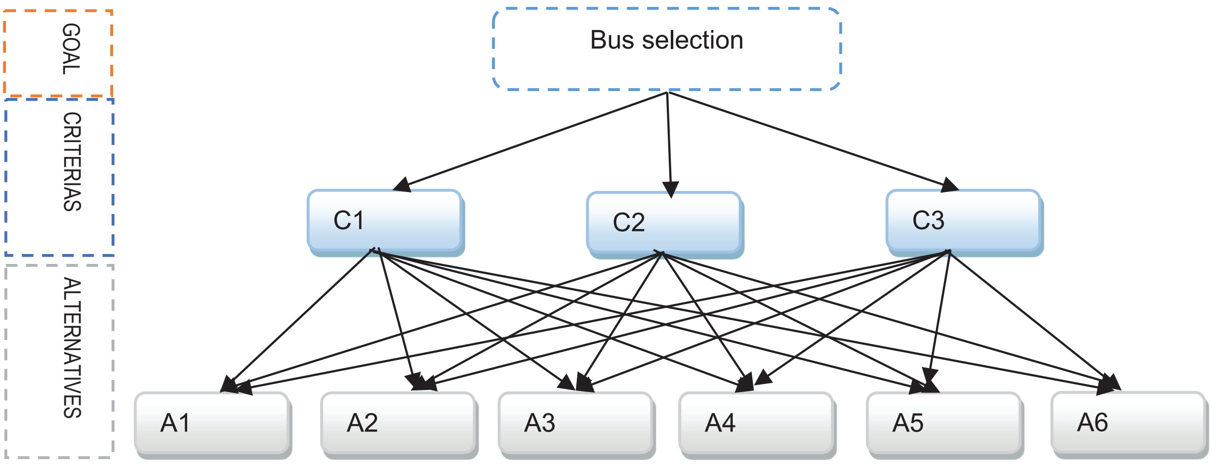

Figure 6. AHP technique (Siksnelyte et al., 2018; Yildiz et al., 2025). AHP, analytic hierarchy process.

Table 4 defines the various options (alternatives) being considered for the decision and the relevant criteria that will be used to evaluate them. For example, if the decision involves choosing the best type of DC microgrid topology, the alternatives might be single-bus, bipolar-bus, ring configurations, multi-bus and multi-terminal topology. The criteria considered in the analysis include protection, resilience, and cost.

Table 5 outlines potential scenarios which consumers classified their individual preferences related to the criteria established in Table 4. These scenarios directly reflect consumer priorities and how they might weigh the different criteria

The AHP avoids directly assigning weights by utilizing pair-wise comparisons. Consumers compare these factors pair-wise, judging which holds more weight for their specific needs. These comparison data are then structured in a matrix, where each cell indicates how much more important one criterion is compared to another, as shown in Table 6.

The pairwise comparison matrix for the criteria, *C*, is: $C = \begin{bmatrix} c_{11} & \cdots & c_{13} \\ \vdots & \ddots & \vdots \\ c_{31} & \cdots & c_{33} \end{bmatrix}$ (11)

Each element of the '**C**' matrix is normalised: $\hat{C} = \left[\hat{C}_{ij}\right] = \left[\frac{C_{ij}}{\sum_{k=1}^{n} C_{kj}}\right]$ (12)

Table 4. Alternatives and criteria

Alternatives	A1	Unipolar microgrid	Figure 1
	A2	Bipolar microgrid	Figure 2
	A3	Ring topology	Wang et al. (2023)
	A4	Multi-terminal topology	Bouchekara et al. (2023)
	A5	Multi-bus topology	Dali et al. (2022)
Criteria	C1	Cost	
	C2	Protection	
	C3	Resilience	

Table 5. Consumer scenarios

Scenarios	S1	S2	S3	S4	5S	S6	S7
Combined criteria	C1 = C2 = C3	C2 > C3 > C1	C2 > C1 > C3	C3 > C2 > C1	C3 > C1 > C2	C1 > C2 > C3	C1 > C3 > C2

Table 6. Saaty's comparison note (Saaty and Vargas, 2012)

Significance level	1	3	5	7	9	2, 4, 6, 8
Definition	Equally important	Moderate important	Strong important	Very strong important	Extreme important	Moderate values

The weight for each criterion is calculated by taking the means of the rows of $\hat{\mathbf{C}}$:

$$W_i = \frac{1}{n}\sum_{j=1}^{n}\hat{C}_{ij} \quad \text{pour } i = 1,\ldots,n \quad \text{with} \sum_{i=1}^{n} w_i = 1 \tag{13}$$

Finally, the AHP method analyses this matrix to calculate weights for each criterion, reflecting their relative influence in the consumer's decision-making, ultimately leading to a DC microgrid selection that prioritises the criteria that matter most to them. The pair-wise comparison matrix (criterion × criterion) considering scenario S5 is defined by Figure 7.

The consistency index and the consistency ratio are calculated by Eqs. (16) and (17).

$$\text{CI} = \frac{\lambda_{\max} - n}{n-1};\ n = \text{number of criteria} \tag{14}$$

$$\text{CR} = \frac{\text{CI}}{\text{random index}\left(RI\right)},\ \text{If CR} < 0.1\text{, pairwise comparison matrix is reasonably consistent.} \tag{15}$$

The pairwise comparison matrix A for the alternatives is: $A = \begin{bmatrix} a_{11} & \cdots & a_{16} \\ \vdots & \ddots & \vdots \\ a_{61} & \cdots & a_{66} \end{bmatrix}$ (16)

Each element of the '**A**' matrix is normalised by: $\hat{a}_{ij}^{(k)} = \frac{a_{ij}^{(k)}}{\sum_{r=1}^{m} a_{ij}^{(k)}}$ (17)

The weight for each alternative is defined by the following relation: $w_i^{(k)} = \frac{1}{m}\sum_{j=1}^{m}\hat{a}_{ij}^{(k)}$ (18)

The pairwise comparison of alternatives for each criterion is presented in Figures 8–10.

	C1	C2	C3	Weight
C1	1	2	0.33	0,263
C2	0.5	1	0.5	0,190
C3	3	2	1	0,547

Figure 7. Criteria's pair-wise comparison from the expert.

Cost (c1)	A1	A2	A3	A4	A5	A6	Wi(C1)
A1	1	2	2	4	4	2	0.32
A2	0.5	1	2	3	3	1	0.2
A3	0.5	0.5	1	2	3	0.5	0.14
A4	0.25	0.33	0.5	1	0.5	0.33	0.06
A5	0.25	0.33	0.33	2	1	0.33	0.08
A6	0.5	1	2	3	3	1	0.2

Figure 8. Cost pair-wise comparisons from all alternatives.

Protection	A1	A2	A3	A4	A5	A6	Wi(C2)
A1	1	2	4	4	4	0.5	0. 31
A2	0.5	1	3	3	3	0.33	0.20
A3	0.25	0.33	1	3	3	0.33	0.12
A4	0.25	0.33	0.33	1	1	0.33	0.06
A5	0.25	0.33	0.33	1	1	0.33	0.06
A6	2	3	3	3	3	1	0.37

Figure 9. Protection pair-wise comparisons from all alternatives.

Resilience(c3)	A1	A2	A3	A4	A5	A6	Wi (C 3)
A1	1	0.25	0.2	0.16	0.16	1	0.10
A2	4	1	2	1	1	3	0.42
A3	5	0.5	1	0.25	0.23	3	0.41
A4	6	1	4	1	0.5	4	0.60
A5	6	1	4	2	1	4	0.61
A6	1	0.33	0.33	0.25	0.25	1	0.11

Figure 10. Resilience pair-wise comparisons from all alternatives.

3.2. Results and Discussion

The analysis shows clear differences in performance between the alternatives. **A2** is the best option, while **A3** is the weakest. The other alternatives fall between these two, as demonstrated in Figure 11.

For scenarios 1, 2, 3, 6 and 7, the unipolar DC microgrid consistently ranked first, while the bipolar DC microgrid consistently held the second position. However, a notable shift occurred in scenarios 4 and 5, where the bipolar DC microgrid surpassed the unipolar DC microgrid to claim the top position. When considering the overall score across all scenarios, the bipolar DC microgrid ultimately secured the second-place ranking, demonstrating its strong overall performance despite the unipolar DC microgrid's dominance in specific scenarios. The multi-terminal topology consistently maintained the lowest ranking across all scenarios, as presented in Figure 12.

When considering all seven scenarios and applying the same approach, the AHP results differ for each scenario. This classification is influenced by the types and number of criteria considered. The bipolar topology emerges as the top choice, followed by unipolar in second place, and AC microgrid in third. It is clear that these rankings are shaped by the specific criteria selected for evaluation. By introducing additional criteria, the rankings could change, potentially leading to a different classification, as presented in Figure 13.

4. AHP sensitivity analysis

4.1. Theoretical Framework

The initial **pairwise comparison matrix** C be an 3×3 matrix, and the initial weight vector is 3 × 1 as given by the next Eq. (19).

$$C=\begin{bmatrix} c_{11} & \cdots & c_{13} \\ \vdots & \ddots & \vdots \\ c_{31} & \cdots & c_{33} \end{bmatrix}, \text{ and } w_C=\begin{bmatrix} w_1 \\ w_2 \\ w_3 \end{bmatrix} \tag{19}$$

Let a small perturbation δc_{ij} be applied to some elements of the judgement matrix C. The perturbed matrix C' is:

$C' = C + \Delta C$; where ΔC represents the matrix of perturbations.

The perturbation in the weight vector will affect the alternative decision matrix D.
The Jacobian matrix, **J** of partial derivatives, is given by Eq. (20).

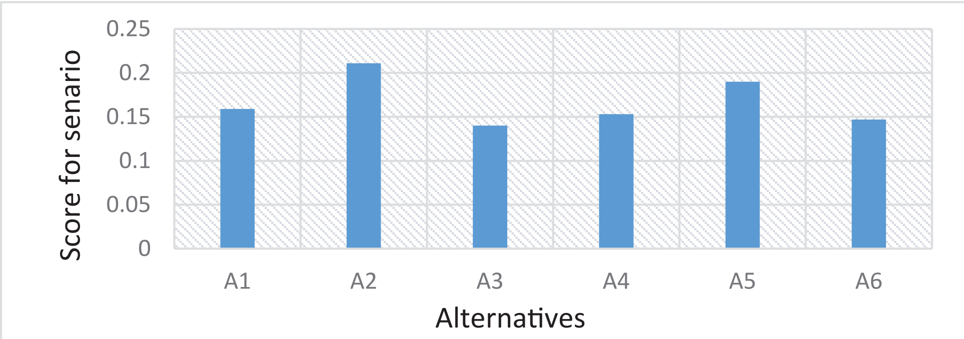

Figure 11. Microgrid scores for scenario 5.

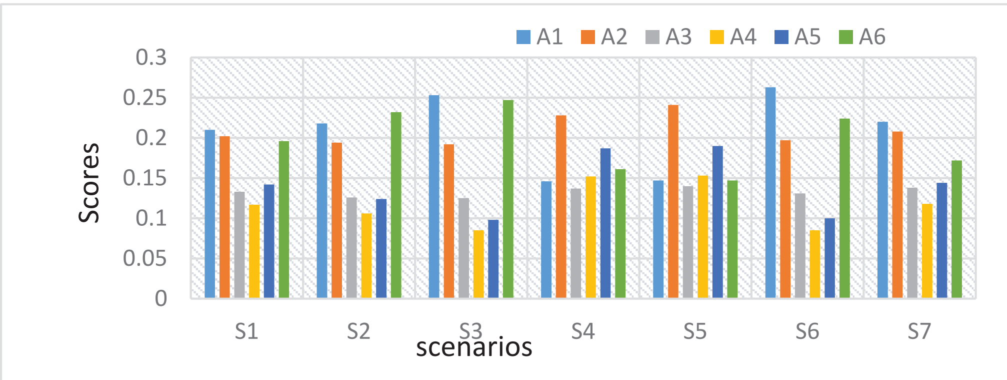

Figure 12. All scenario results.

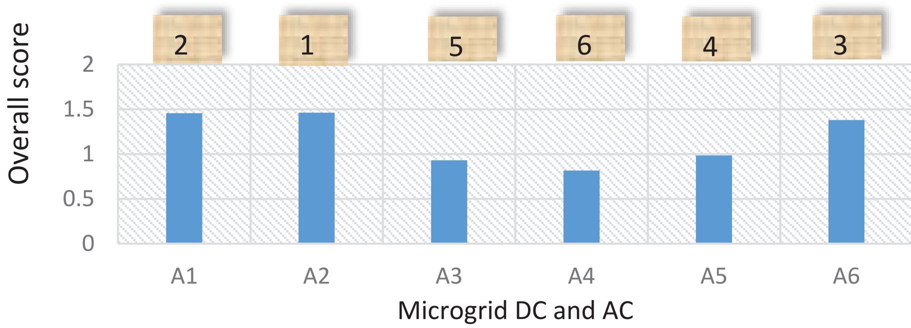

Figure 13. Overall score for each microgrid topology.

$$J = \frac{\partial D}{\partial C} = \begin{bmatrix} D_{1/C1} & D_{1/C2} & D_{1/C3} \\ D_{2/C1} & D_{2/C2} & D_{2/C3} \\ D_{3/C1} & D_{3/C2} & D_{3/C3} \\ D_{4/C1} & D_{4/C2} & D_{4/C3} \\ D_{5/C1} & D_{5/C2} & D_{5/C3} \\ D_{6/C1} & D_{6/C2} & D_{6/C3} \end{bmatrix} \tag{20}$$

where: $\frac{\partial D_i}{\partial C_j}$ is the partial derivative of the decision with respect to the pairwise comparison judgement between alternatives *i* and criteria *j*.

A large value for $\frac{\partial D_i}{\partial C_j}$ indicates that a small change in the criteria (*j*) can greatly affect the alternative (*i*) rank. On the contrary, a small value means that the decision is less sensitive to changes in the criteria (*j*)weight.

4.2. Results and discussion

4.2.1. Sensitivity performance analysis

This analysis presents simulation results generated using Expert Choice software to assess the impact of various factors on the decision-making process.

In Figure14, the weight of each criterion is represented by a vertical bar, with its value indicated on the left-hand y-axis. The height of each bar represents the relative importance. For example, for the risk factor 'resilience', a value of 60% is read on the left-hand y-axis. The extension of each vertical line of the risk factors to the intersection with the curve of each alternative indicates on the right-hand y-axis. For example, for the risk factor 'cost', the intersection of the vertical line with the undesirable results A6, A5, A4, A3, A2 and A1 indicates preferences of 52%, 17%, 20%, 35%, 52% and 78%, respectively. Moreover, it is clear that the undesirable result for the alternative 'AC microgrid' (pink curve) is predominant for the 'protection' factor, the undesirable result for the alternative 'multi-bus topology' (green curve) is predominant for the 'resilience' factor and the undesirable result for the alternative 'unipolar DC microgrid' (blue curve) is predominant for the 'cost' factor. Furthermore, the overall preference (OVERALL) indicates that the undesirable consequence of 'ring topology' is globally prevalent in the analysis for all three risk factors.

4.2.2. Gradient sensitivity analysis

Gradient sensitivity analyses were performed for each risk factor to assess its individual influence on the undesirable results. To enhance interpretability, the focus will be on the first and second-ranked alternatives, analysing how their rankings change when criterion weights are varied.

The accompanying Figure 15 depicts the sensitivity gradient for the 'protection' criterion. The impact of varying the criterion weight within the ranges of 0%–45% and 45%–100% was analysed. Despite adjustments to the criterion weight, the 'bipolar DC microgrid' consistently maintained its top ranking. However, within the 50%–100% range, the 'unipolar DC microgrid' surpassed the 'bipolar DC microgrid' to claim the second position, and the first position is to AC microgrid.

A similar sensitivity analysis was conducted for the 'cost' criterion, revealing that the 'bipolar DC microgrid' lost its top ranking to the 'AC microgrid' when the 'cost' weight exceeded 50%, as shown in Figure 16.

The sensitivity analysis for the 'resilience' criterion revealed three distinct intervals: (1) 0%–30%, where the 'AC microgrid' and 'unipolar DC microgrid' maintained the first and second ranking; (2) 30%–65%, where the 'bipolar DC microgrid' became the preferred choice as shown in Figure 17.

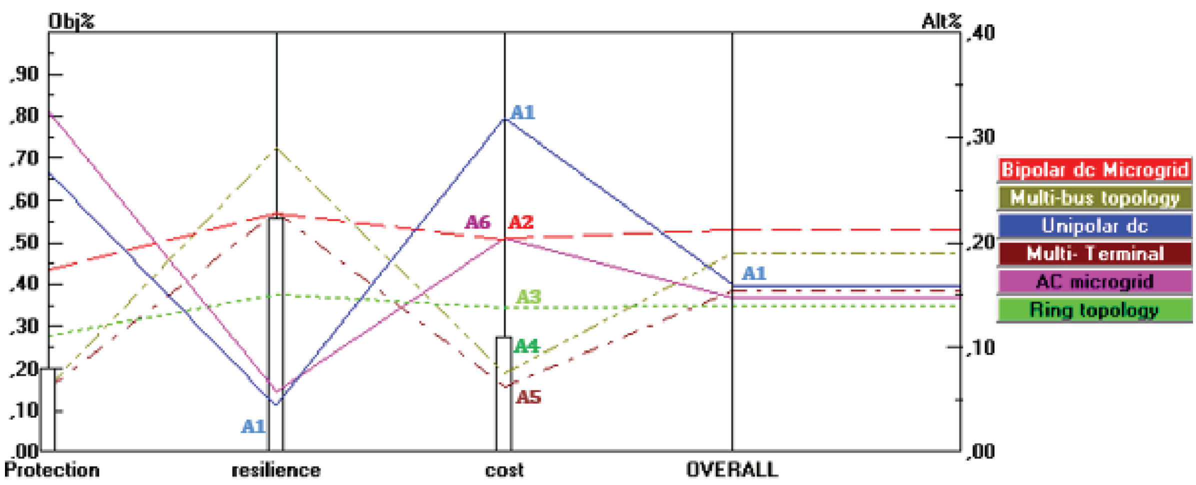

Figure 14. Performance sensitivity of the alternative.

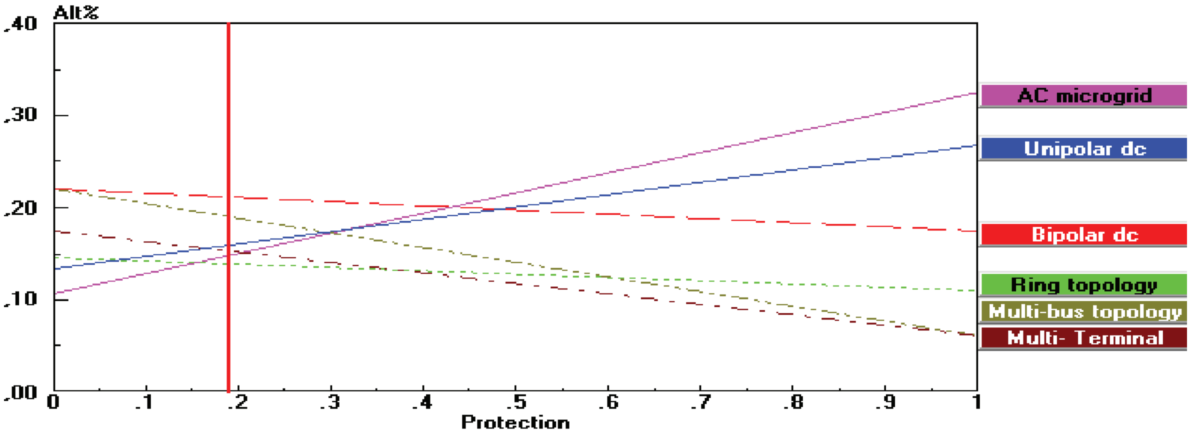

Figure 15. Protection gradient sensitivity.

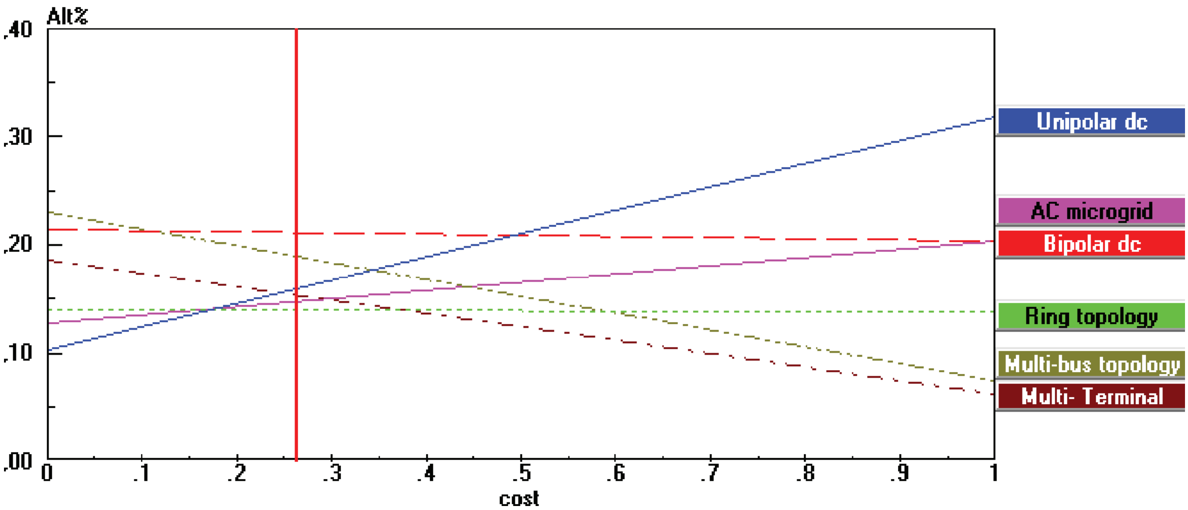

Figure 16. Cost gradient sensitivity.

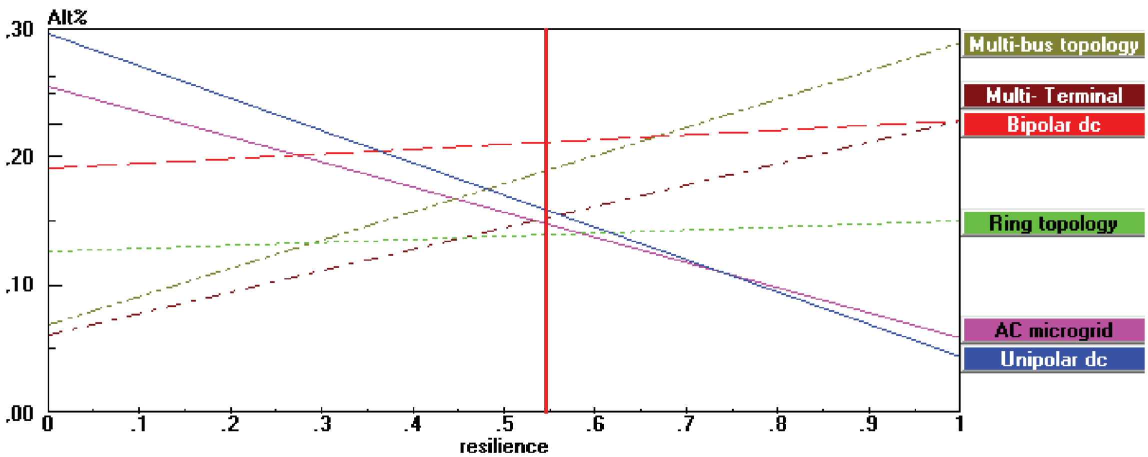

Figure 17. Resilience gradient sensitivity.

Using the three graphs Figures 15–17, the equation for each alternative can be determined by applying interpolation to each segment of the curve. The resulting decision matrix is given by:

$$D_{\exp} = \begin{bmatrix} D_{1/C1} & D_{1/C2} & D_{1/C3} \\ D_{2/C1} & D_{2/C2} & D_{2/C3} \\ D_{3/C1} & D_{3/C2} & D_{3/C3} \\ D_{4/C1} & D_{4/C2} & D_{4/C3} \\ D_{5/C1} & D_{5/C2} & D_{5/C3} \\ D_{6/C1} & D_{6/C2} & D_{6/C3} \end{bmatrix} = \begin{bmatrix} 0.26x+0.10 & 0.13x+0.15 & -0.20x+0.29 \\ 0.01x+0.21 & -0.01x+0.22 & 0.03x+0.20 \\ -0.02x+0.16 & -0.07x+0.17 & 0.13 \\ -0.11x+0.22 & -0.06x+0.14 & 0.12x+0.07 \\ -0.18x+0.26 & -0.06x+0.13 & 0.20x+0.07 \\ -0.09x+0.19 & 0.25x+0.12 & -0.16x+0.26 \end{bmatrix} \tag{21}$$

Then, the Jacobian matrix, *J*, will be equal to:

$$J_{\exp} = \frac{\partial D_{\exp}}{\partial C_i} = \begin{bmatrix} 0.26 & 0.13 & -0.20 \\ 0.01 & -0.01 & 0.03 \\ -0.02 & -0.07 & 0.13 \\ -0.11 & -0.06 & 0.12 \\ -0.18 & -0.06 & 0.20 \\ -0.09 & 0.25 & -0.16 \end{bmatrix} \tag{22}$$

The Decision Expert Matrix analysis indicates that alternatives 1, 5 and 6 exhibit high sensitivity to variations in criteria weights, suggesting potential instability in their rankings. Alternative 4 demonstrates a moderate level of sensitivity, while alternatives 2 and 3 show the least sensitivity and the highest stability. This highlights that the rankings of alternatives (1,5,6) are significantly influenced by weighting adjustments, whereas alternatives 2 and 3 remain more robust and reliable under different weighting scenarios.

5. Sensitivity Improving

5.1. Analytic method

To improve the quality of the research, a dual-source data acquisition strategy is employed. The first dataset is based on expert evaluations, informed by their specialised knowledge. The second dataset is derived from established scientific literature. By integrating these complementary data sources, a more comprehensive and reliable assessment is achieved. Table 7 provides a review of microgrid criteria and their importance across different topologies (Al Dawsari et al., 2024; Cabana-Jiménez et al., 2022; Gerber et al., 2023; Kiptoo et al., 2023).

The analysis of Table 7 indicates that DC microgrid research places the highest priority on resilience (40%), underscoring the critical need for systems capable of withstanding disruptions. Protection ranks second at 30%, emphasizing the importance of safeguarding equipment and ensuring safety. Cost, while still a key factor, holds

Table 7. Data from scientific articles

Criterion alternatives	Cost (20%)	Short-circuit resilience (40%)	Protection complexity (30%)
Unipolar DC MG	Economical for basic setups	Limited	Low
Bipolar DC MG	Moderate	Enhanced redundancy (20%)	Moderate
Ring topology	Moderate	Self-healing capabilities (30%)	Moderate
Multi-terminal	High	Adaptive energy management (20%)	High
Multi-bus	High	Fault isolation and modular replacement (30%)	High

Database: IEEE Xplore, MDPI Energies Science Direct, IET Renewable Power Generation Period Jan 2015–Dec 2023 a lower priority (20%), suggesting that it is optimised within the constraints defined by resilience and protection requirements (Bouchekara et al., 2023; Chandra et al., 2020). The pairwise comparison matrix is presented in Figure 18.

The second criterion has the highest weight, which is also observed in the expert judgement. However, the first and last criteria change in the expert judgement results. The results of both tables are closely comparable, though variations may occur if more criteria are introduced. The method used to improve the sensitivity of the decision matrix is illustrated in Figure 19.

The decision matrix based on scientific data can be determined using expert choice software results.

$$D_{SC} = \begin{bmatrix} 0.17x+0.15 & 0.10x+0.16 & -0.26x+0.29 \\ 0.21 & -0.02x+0.21 & 0.03x+0.19 \\ 0.13 & -0.04x+0.15 & 0.02x+0.14 \\ -0.12x+0.18 & -0.15x+0.22 & 0.17x+0.06 \\ -0.02x+0.18 & -0.11x+0.17 & -0.23x+0.28 \\ 0.20 & 0.21x+0.11 & -0.23x+0.29 \end{bmatrix} \tag{23}$$

Then, the Jacobian matrix from scientific data J_{sc} will be equal to:

$$J_{sc} = \frac{\partial D_{sc}}{\partial C_i} = \begin{bmatrix} 0.17 & 0.10 & -0.26 \\ 0 & -0.02 & 0.03 \\ 0 & -0.04 & 0.02 \\ -0.12 & -0.15 & 0.17 \\ -0.02 & -0.11 & -0.23 \\ 0 & 0.21 & -0.23 \end{bmatrix} \tag{24}$$

The global Jacobian matrix from all data will be equal to:

$$J = a\frac{\partial D_{exp}}{\partial C_i} + \mathrm{b}\frac{\partial D_{sc}}{\partial C_i} = \begin{bmatrix} 0.26a+0.17b & 0.13a+0.10b & -0.20a-0.26b \\ 0.01a & -0.02a & -0.11a-0.12b \\ -0.18a-0.02b & -0.09a & -0.01a-0.02b \\ -0.07a & -0.06a-0.15b & -0.06a-0.11b \\ 0.25a+0.21b & 0.03a+0.03b & 0.13a+0.02b \\ 0.12a+0.17b & 0.20a-0.23b & -0.16a-0.23b \end{bmatrix} \tag{25}$$

Given that a and b are weighting coefficients that represent the relative importance of expert judgements and scientific data in assessing the impact of a change on the sensitivity of a decision, a sensitivity analysis can be

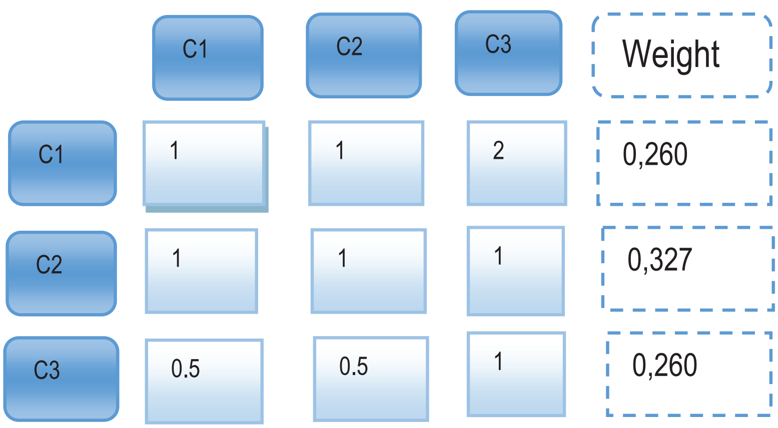

Figure 18. Pairwise comparison matrix from scientific articles.

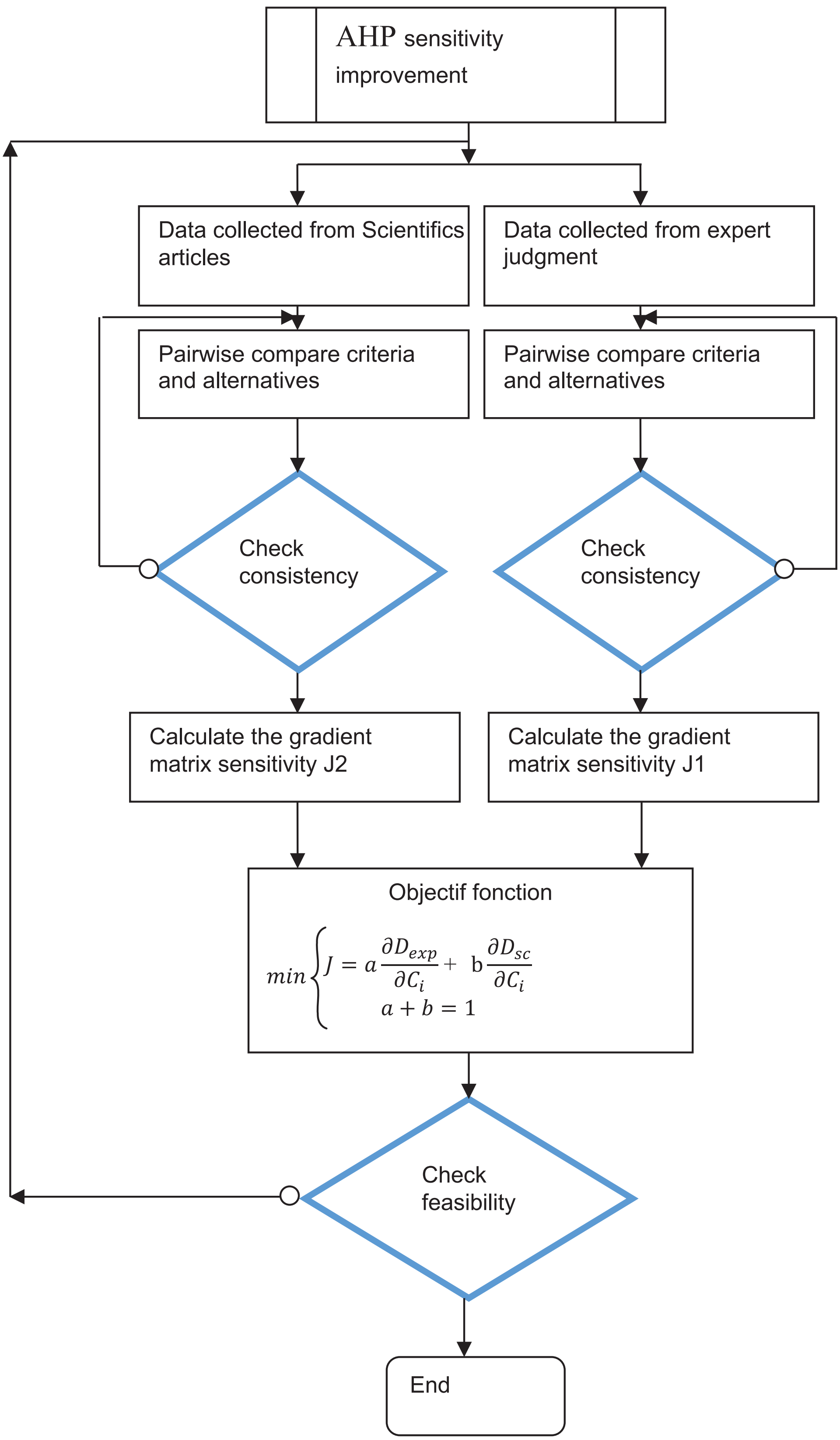

Figure 19. Flowchart of sensitivity improvement. AHP, analytic hierarchy process.

conducted. The goal is to determine a and b while minimizing the elements of the global Jacobian matrix. To achieve this, the Frobenius norm of the matrix is used. The Frobenius norm is given by:

$$\|J\|_F = \sqrt{\sum_{i,j} |J_{ij}|^2} \tag{26}$$

where J_{ij} are the elements of the matrix J. The Frobenius norm squared is:

$$\| J \|_F^2 = 0.8376a^2 + ab + 0.8048b^2 \tag{27}$$

The objective function to minimise is:

$$f(a,b) = 0.8376a^2 + ab + 0.8048b^2$$

Subject to the constraint:

$$g(a,b) = a + b - 1 = 0 \tag{28}$$

The evolution of the norm of Frobenius is presented by Figure 20.

These values that minimise the Frobenius norm of the matrix J under the constraint are:

$$a \approx 0.4745, \quad b \approx 0.5255$$

This approach reflects the understanding that scientific data, often gathered through rigorous research and analysis, tends to be more consistent and objective compared to expert judgement, which may be influenced by personal biases or limited experience.

By prioritizing scientific data, we are reducing the risk of decisions being overly influenced by subjective factors. This adjustment ensures that the results of the AHP model are more robust and less sensitive to variations in expert opinions. Moreover, this approach plays a key role in improving the sensitivity of the final decision.

5.2. Results and discussion

Figure 21 presents the ranking of six alternatives (A1–A6) under three conditions: initial ranking, after criteria weight perturbation, and after optimisation. It visually compares how the ranks shift across these scenarios.

The initial ranking shows A2 as the top alternative and A3 as the lowest. After criteria weight perturbation, all alternatives shift in rank, with A1 falling to first place, indicating high sensitivity. Alternatives A4 and A5 show a decrease, indicating that the new weight setup is less favourable for them. The optimisation process restores rank stability, with most alternatives returning to positions close to the initial scenario. A2 regains the top position, and A1, A3, and A5 also align with their original ranks. Only A4 and A6 switch places, showing minor impact and confirming the optimisation's effectiveness in stabilizing the decision.

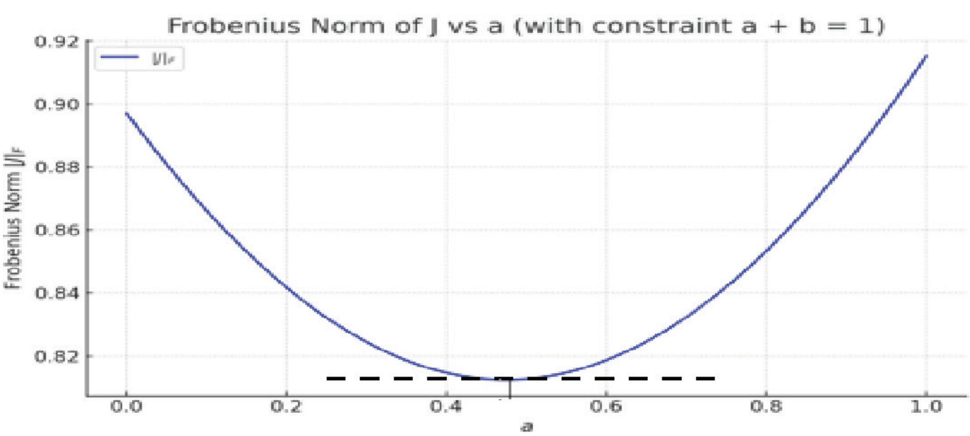

Figure 20. Frobenius norm evolution.

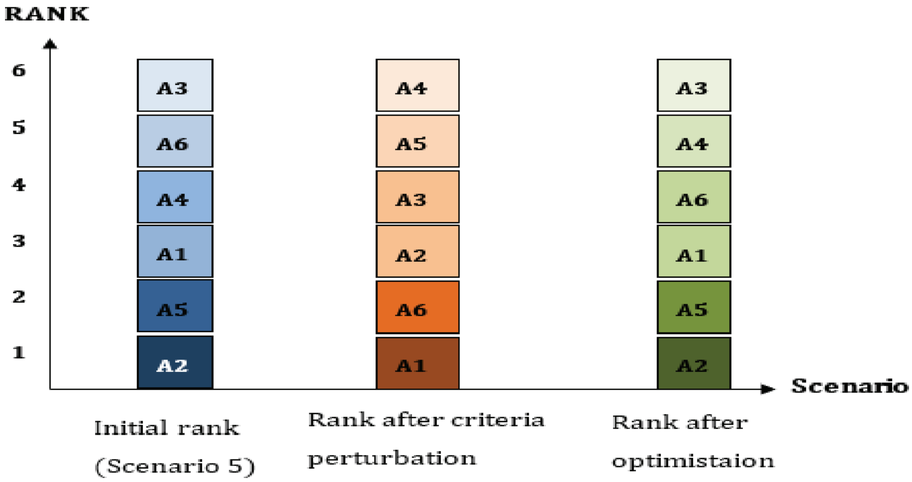

Figure 21. Rank of decision vector.

6. Conclusion

This comparative analysis, employing the MCDA AHP methodology, evaluated various DC microgrid topologies considering key factors such as protection, resilience, and cost. The results consistently demonstrated the superiority of the DC bipolar microgrid, reinforcing its potential for standardisation and widespread adoption. Enhancing the sensitivity analysis by incorporating diverse data sources, such as expert opinions and scientific literature, can further minimise result variability. This approach would refine the resolution of the objective function, ensuring more accurate and reliable evaluations. By integrating both empirical insights and theoretical knowledge, the robustness and credibility of the analysis can be significantly strengthened, paving the way for more informed decision-making in microgrid design and implementation. Furthermore, the incorporation of optimisation algorithms enhances sensitivity handling, improves the precision of weight calibration, and ensures that the final decision vector is more stable and robust.

References

Al Dawsari, S., Anayi, F. and Packianather, M. (2024). Techno-Economic Analysis of Hybrid Renewable Energy Systems for Cost Reduction and Reliability Improvement Using Dwarf Mongoose Optimization Algorithm. *Energy*, 313, p. 133653. doi: 10.1016/j.energy.2024.133653

Beyza, J. and Yusta, J. M. (2021). Integrated Risk Assessment for Robustness Evaluation and Resilience Optimisation of Power Systems After Cascading Failures. *Energies*, 14(7), p. 2028. doi: 10.3390/en14072028

Böhringer, C., Cuntz, A., Harhoff, D. and Asane-Otoo, E. (2017). The Impact of the German Feed-in Tariff Scheme on Innovation: Evidence Based on Patent Filings in Renewable Energy Technologies. *Energy Economics*, 67, pp. 545–553. doi: 10.1016/j.eneco.2017.09.001

Bouchekara, H. R., Sha'aban, Y. A., Shahriar, M. S., Abdullah, S. M. and Ramli, M. A. (2023). Sizing of Hybrid PV/Battery/Wind/Diesel Microgrid System Using an Improved Decomposition Multi-Objective Evolutionary Algorithm Considering Uncertainties and Battery Degradation. *Sustainability*, 15(14), p. 11073. doi: 10.3390/su151411073

Cabana-Jiménez, K., Candelo-Becerra, J. E. and Sousa Santos, V. (2022). Comprehensive Analysis of Microgrids Configurations and Topologies. *Sustainability*, 14(3), p. 1056. doi: 10.3390/su14031056

Chandra, A., Singh, G. K. and Pant, V. (2020). Protection Techniques for DC Microgrid—A Review. *Electric Power Systems Research*, 187, p. 106439. doi: 10.1016/j.epsr.2020.106439

Chang, F., Cui, X., Wang, M. and Su, W. (2021). Potential-Based Large-Signal Stability Analysis in DC Power Grids with Multiple Constant Power Loads. *IEEE Open Access Journal of Power and Energy*, 9, pp. 16–28. doi: 10.1109/OAJPE.2021.3132860

Dali, M., Charaabi, F. and Belhadj, J. (2022, October). Short-circuit fault analysis and protection of stand-alone AC and DC microgrids. In: *2022 IEEE International Conference on Electrical Sciences and Technologies in Maghreb (CISTEM)*. IEEE, Institut National des Sciences Appliquées et de Technologie Tunisia. (INSAT), Vol. 4, pp. 1–6.

Eskander, M. M. and Silva, C. A. (2023). Techno-Economic and Environmental Comparative Analysis for DC Microgrids in Households: Portuguese and French Household Case Study. *Applied Energy*, 349, p. 121495. doi: 10.1016/j.apenergy.2023.121495

Feng, W., Jin, M., Liu, X., Bao, Y., Marnay, C., Yao, C. and Yu, J. (2018). A Review of Microgrid Development in the United States—A Decade of Progress on Policies, Demonstrations, Controls, and Software Tools. *Applied Energy*, 228, pp. 1656–1668. doi: 10.1016/j.apenergy.2018.06.096

Gerber, D. L., Nordman, B., Brown, R. and Poon, J. (2023). Cost Analysis of Distributed Storage in AC and DC Microgrids. *Applied Energy*, 344, p. 121218. doi: 10.1016/j.apenergy.2023.121218

Jena, K., Panigrahi, C. K. and Gupta, K. K. (2021). A New 13-Level Switched-Capacitor Inverter with Reduced Device Count. *Power Electronics and Drives*, 6, pp. 26–41. doi: 10.2478/pead-2021-0005

Kiptoo, M. K., Adewuyi, O. B., Furukakoi, M., Mandal, P. and Senjyu, T. (2023). Integrated Multi-Criteria Planning for Resilient Renewable Energy-Based Microgrid Considering Advanced Demand Response and Uncertainty. *Energies*, 16(19), p. 6838. doi: 10.3390/en16196838

Kumar, A. A. and Prabha, N. A. (2022). A Comprehensive Review of DC Microgrid in Market Segments and Control Technique. *Heliyon*, 8, p. e11694. doi: 10.1016/j.heliyon.2022.e11694

Meddeb, A., Sahbeni, N., Jmii, H., and Chebbi, S. (2018, March). Impact of distributed generation on the protection system in Tunisian distribution network. In: *2018 15th International Multi-Conference on Systems, Signals & Devices (SSD)*. IEEE, Yasmine Hammamet, Tunisia, pp. 514–520.

Mohamed, A., Refaat, S. S. and Abu-Rub, H. (2019). A Review on Big Data Management and Decision-Making in Smart Grid. *Power Electronics and Drives*, 4(39), pp. 1–13. doi: 10.2478/pead-2019-0011

Parvaneh, F. and Hammad, A. (2024). Application of Multi-Criteria Decision-Making (MCDM) to Select the Most Sustainable Power-Generating Technology. *Sustainability*, 16(8), p. 3287. doi: 10.3390/su16083287

Punitha, S., Subramaniam, N. P. and Vimal Raj, P. A. D. (2024). A Comprehensive Review of Microgrid Challenges in Architectures, Mitigation Approaches, and Future Directions. *Journal of Electrical Systems and Information Technology*, 11(1), p. 60. doi: 10.1186/s43067-024-00188-4

Rocchetta, R., Zio, E. and Patelli, E. (2018). A Power-Flow Emulator Approach for Resilience Assessment of Repairable Power Grids Subject to Weather-Induced Failures and Data Deficiency. *Applied Energy*, 210, pp. 339–350. doi: 10.1016/j.apenergy.2017.10.126

Saaty, T. L. (2008). Decision Making with the Analytic Hierarchy Process. *International Journal of Services Sciences*, 1(1), pp. 83–98. doi: 10.1504/IJSSCI.2008.017590

Saaty, T. L. and Vargas, L. G. (2012). *Models, Methods, Concepts & Applications of the Analytic Hierarchy Process*. Springer Science & Business Media, New York.

Siksnelyte, I., Zavadskas, E. K., Streimikiene, D. and Sharma, D. (2018). An Overview of Multi-Criteria Decision-Making Methods in Dealing with Sustainable Energy Development Issues. *Energies*, 11(10), p. 2754. doi: 10.3390/en11102754

Wang, F., Tian, J., Ling, J., Chen, Z. and Xu, Z. (2025). A Multi-Stage Resilience Analysis Framework of Critical Infrastructure Systems Based on Component Importance Measures. *Reliability Engineering & System Safety*, 256, p. 110720. doi: 10.1016/j.ress.2024.110720

Wang, H., Yan, S., Ju, D., Ma, N., Fang, J., Wang, S., Li, H., Zhang, T., Xie, Y. and Wang, J. (2023). Short-Term Photovoltaic Power Forecasting Based on A Feature Rise-Dimensional Two-Layer Ensemble Learning Model. *Sustainability*, 15(21), p. 15594. doi: 10.3390/su152115594

Yildiz, O. A., Cebi, S. and Yildiz, O. (2025). Multicriteria Decision Support for Sustainable Energy Planning: An Evaluation of Alternative Scenarios for the Solar Power Plant Site Selection. *Environment, Development and Sustainability*, pp. 1–35. doi: 10.1007/s10668-024-05943-1.

Yodo, N. and Wang, P. (2016). Engineering Resilience Quantification and System Design Implications: A Literature Survey. *Journal of Mechanical Design*, 138(11), p. 111408. doi: 10.1115/1.4034223